Quantum Time Signals in Living Beings

Brad Eckert

Abstract—We treat consciousness as a physical process occuring inside and outside of time simultaneously, per spiritual traditions and recent scientific advances. This view requires two dimensions of time. Quantum time emerges from consciousness as it interacts with both worlds. The relationship between the time dimensions provides a mechanism for apparent noise arising from both our biological signaling and connection to divinity. We present an algorithm for the demodulation of white and flicker noise, which can have discernible information content that instruments the mind-body landscape. The demodulated signals facilitate a new class of consciousness applications. The detection and analysis of these signals has far-reaching implications for determinism, free will, heritability, health, and human interconnectedness.

Index Terms—Tao, noise, quantum time, relative time, consciousness, QTDSP.

◆

1 Two-Dimensional Time

According to many spiritual traditions, including yogic ones that rely on direct observation through meditation, the consciousness of humans, animals, and all living things is a combination of the finite and the infinite, existing both inside and outside of material reality. Allowing more than one dimension of time theoretically supports this view of existence beyond the material world. The existence of non-local mind effects, since they hold up under serious investigation [1], provides a real impetus for multi-dimensional time.

Investigation of 2D time with an eye toward practical instrumentation has the potential of bearing the kind of fruit necessary to heal the schism between science and religion. Standing on the shoulders of giants provides a good starting point.

The Wheeler-DeWitt equation [2] attempts to combine mathematically the ideas of quantum mechanics and general relativity. One of its implications is the "problem of time", which is a conceptual conflict between general relativity and quantum mechanics. Quantum mechanics regards the flow of time as universal and absolute, whereas general relativity regards the flow of time as malleable and relative.

According to Wheeler-DeWitt, an observer outside of the universe doesn't experience time. Page and Wootters [3] addressed this paradox (time *seems* real enough) by treating time as an emergent phenomenon resulting from quantum entanglement. Experiments [4] on entangled particles have bolstered the theory.

There are other takes on timeless universe models. Aharonov's two state formalism of quantum mechanics has also been used [5] to propose emergence of time from a timeless unus mundus quantum-like space. Jianfeng Li provides a good overview [6] of quantum mechanical timeless consciousness.

There are two distinct types of time: emergent time, which emanates from the structure of space-time and its metrics, and a causal time, indicating the flow from the past to the future [7]. The time domains relate the two models of Physics, QM and GR. In the interest of a nomenclature, we call one dimension of time the quantum time domain and the other the relative time domain. So, *quantum time* and *relative time*. Relative time is the one with the arrow.

The hard problem of consciousness [8] is that of explaining the relationship between physical phenomena, such as brain processes, and experience. Experiments in non-locality [9] find that the mind extends beyond the skull. Where is the mind, inside space-time or outside? The evidence suggests it is both.

Our everyday experience is that "clock time" is the reference frame, although it could just as well be that quantum time is the existential norm and the "clock time" universe is a special case. We take the view of quantum time observed from within the universe, with the observation being an act of quantum entanglement caused by consciousness.

1.1 Quantum Time and Consciousness

There are many examples of biological systems exploiting quantum effects. Nature would have evolved to exploit the properties of quantum time.

The physical vacuum, a substrate for quantum interactions, is a natural mechanism for biological systems to have evolved to utilize. Consciousness is the interaction between the physical vacuum and biology which facilitates communication at any physical scale, from DNA to organism.

This provides an important signaling mechanism for consciousness in beings such as paramecia or slime molds, which exhibit conscious behavior but are too small for consciousness to arise from the network effects of ganglia.

One way to relate the two time dimensions is with a scale-invariant geometry that exploits the simplicity of self-similarity. As Mandelbrot [10] pointed out, relatively simple fractal mathematics underlie many complex natural phenomena. As it turns out, this exponential relationship between τ and t is a key enabler of signal transformations.

For it to be scale invariant, we use an exponential growth model for quantum time.

$$\tau \propto e^{\epsilon t} \tag{1}$$

The mechanics of signal generation can be considered in the context of quantum time. This arrangement lends itself to information flow, utilized by nature, between the time and timeless domains.

Resonance is treated as a physical phenomenon occurring in quantum time τ. A resonant frequency in τ is equivalent to an exponential chirp in t. This dynamic emergence of time should produce small but detectable artifacts. The stream of consciousness emerges from a probabilistic field on an exponential time scale rather than time abruptly appearing from nothing.

Biological systems evolve to minimize the expenditure of energy. Resonances (field analogs of electrical and mechanical ringing) require a small energy input to keep them going, assuming a reasonably high Q. It stands to reason that biological systems would use field resonances in the physical vacuum (the exact nature of the field needs not be understood) to transmit consciousness information efficiently.

In other words, there is a theoretical basis for the notion that "It's all vibrations". The vibrations occur in quantum time, so their signal artifacts produce a noise spectrum. Of course, nature is never simple. There could be other dimensions at play or even backward time effects providing the excitation for the resonance. Since we're only looking for artifacts, the details aren't as important as verifying the existence of the artifacts in the first place.

The signals that encode this information can be demodulated from "noise".

Quantum time allows for "randomness" in a non-deterministic, panentheistic Universe. In other words, a form of Leibnizian Idealism [11]. For example, if we are living in a simulation then noise is pseudorandom and there is no true randomness.

2 EXPONENTIAL FLICKER NOISE

Flicker noise (or 1/f noise), has a power spectrum proportional to $1/f^{\alpha}$, where α is between 0.7 and 1.4. It's a type of noise prevalent in many natural systems. Flicker noise [12] is seen in music, seismic data, EEG and ECG data, and electronic devices. Some of the more popular explanations for the 1/f spectrum are:

- A superposition of relaxation processes.
- Carrier mobility fluctuations through Coulomb scattering.

There are a good number of hypotheses for 1/f noise, to which we add one more:

- The superposition of exponential chirps.

An exponential swept-sine signal with constant amplitude has a power spectrum [13] that is constant-slope (on a log-log plot) at roughly -6dB per octave, curiously similar to a flicker noise power spectrum. This is independent of "warp factor" ω.

$$Signal \propto sin(k \cdot e^{\omega t}) \tag{2}$$

2.1 Exponential White Noise

White noise has a flat power spectrum. In a white noise model of quantum time, chirps start at 0 and asymptotically approach a final frequency as quantum time merges into relative time.

$$\frac{1}{\tau} \propto (1 - e^{-\epsilon t}) \tag{3}$$

In other words, the consciousness signal emerges from a domain of infinite time. The power drops off at the same rate frequency increases, resulting in a flat spectrum from DC to f_0.

$$f = f_0 \cdot (1 - e^{-\epsilon t}) \tag{4}$$

$$p = p_0 \cdot e^{-\epsilon t} \tag{5}$$

f_0 would be millimeter wave (such as 60 GHz oxygen resonances) and higher. Terahertz (mostly in the 600 THz range) oscillations in tubulin [14] correlate with anesthetic potency, which opens the possibility that tubulin oscillations are carriers of consciousness information.

The chirp would mix with carrier f_0 to produce a downward chirp (assuming the signal is moving forward in time) with power dropping with frequency, which flattens out the spectrum so it's still white. The resulting chirp signal is more practical due to the shortness of the time the chirp itself spends in a bandwidth that lends itself to detection.

The amplitude droop may be compensated for in the input warping stage. White noise follows the same rules as pink noise except for the spectral bias.

2.2 Information in the Noise

Since exponential chirps are bounded in time, a single chirp has a finite existence. It corresponds to a discrete impulse in the relative time domain, or one symbol of information. The idea of consciousness as time quanta may be useful here. The act of being is a stream of consciousness that has corresponding streams of pulse-coded information, a kind of informational counterpart to DNA. The impulse stream may be decoded for its information content. The detection of an impulse stream itself is valuable, regardless of our initial ability to decode it, because useful information can be mined from its distribution of ω values.

Consciousness quanta have a foundation in Penrose and Hameroff's "Orch OR Theory" [15]. In objective reduction, the divergence of quantum superposition in the underlying structure of the universe builds to the point of collapse, or objective reduction of the quantum state. Each collapse is a moment of conscious experience. In "Orch OR", EEG data is a macro view of these moments. EEG has both a flicker noise spectrum and frequency peaks that correspond to "Orch OR" collapse. There is already much scientific data (such as EEG and ECG studies) in the public domain, ready to analyze. The experimental costs are low: mostly computer hardware.

Overlapping chirps can be re-sampled and self-correlated to construct a relative time domain signal for one or a multiplicity of ω values. A sweep of ω can be used to construct a "warp spectrum" (for example, on a computer display), useful for finding quantum-time signals.

This would be analogous to waterfall-style spectral analysis, with frequency replaced by warp factor.

To establish a notation and unit of measurement for quantum frequency, let the "warp factor" ω be in units of e, the mathematical constant derived by Leonhard Euler in the 1720s, per unit time. The pronunciation may be "e's per second" for e/s, for example. We propose "len" for the unit name of e/s, after Leonhard. Some scale factors to other units: 0.69 lens is one octave per second, 2.3 lens is one order per second, and 0.48 lens is one golden mean ($\Phi = 1.618 : 1$) per second. Note that a len is very close to twice the Golden Ratio, so one must be careful when making assumptions about Golden Ratio relationships in nature.

2.3 Spiral Conceptual Model

Fig. 1. Log polar plot of exponential chirp

Resonant signals in the quantum time domain can be re-mapped to relative time and demodulated by correlating a series of fast exponential chirp transforms, allowing analysis and data mining using modern data processing technologies such as AI-based pattern recognition.

The correlation effect can be visualized as a spinning logarithmic spiral illuminated by a strobe light. When the strobe frequency matches the rate constant of the spiral(s), it appears to be standing still. Otherwise, it's a blur.

The relationship between quantum time and relative time can be thought of as a 2D plot in log-polar format. Log-polar format renders a logarithmic spiral as a linear (Archimedean) spiral. The spiral's radius is $\rho = k\theta$, where k is a rate constant. ρ can represent either time or frequency by flipping the sign of k. For purposes of signal processing, let ρ represent log frequency and θ relative time.

Log-polar mapping has proven useful in machine vision [16] because it approximates the primate visual map [17]. Humans are visual thinkers, so their waking consciousness should map onto the log-polar structure of quantum time signaling.

Fig. 1 plots an exponential chirp in log-polar format. A line can be drawn outward from the center of the spiral, crossing it at multiple points. The line rotates clockwise (in the case of downward chirp) at a step size (from t_1 to t_2) corresponding to the oversampling rate. For example, if the oversampling rate is 36 (each input value is used 36 times),

Fig. 2. Inter-domain data flow

the step size is $10°$. Each angular sweep of the unit circle (beginning and ending at line t_1 or t_2) represents the input to a version of the Mellin transform called the "Exponential Chirp Transform" (ECT) [16], which is basically a FFT with time-warped input.

The transform's frequency domain output is along line t_1 or t_2 from approximately $\rho = 0$ to Fs/2, where Fs/2 (the Nyquist frequency) is shown by the dashed circle. The radius of the circle represents the approximate bandwidth of the system. Not all of the circle is used: Anti-aliasing cuts off before Fs/2, while signal near the center is too spread out to be useful.

The ECT time-warps the chirp signal, which represents a single "quantum tone". In the $360°$ sweep at line t_1, the chirp is time-warped to a tone F1 in relative time. A time $t_2 - t_1$ later, at line t_2, it's time-warped to a tone of frequency F2. All time warping is exponential. Note that "exponential time warping" is different from dynamic time warping, a popular means of pattern-matching mostly linear signals.

A convenient side effect of time warping is to transform interference (periodic signals) into wideband noise. The usual frequency peaks of EEG and HRV are thus discarded.

Quantum time, being logarithmic, has the property of frequency going as $-\tau$ rather than $1/t$. To change between time and frequency, just flip the sign of the exponent. Tones are mirror images of time. Signal processing is more convenient in terms of frequency, so that is the focus of this paper.

2.4 Quantum Time DSP

The basic data flow of signal conversion from one time domain to another ($\tau \leftrightarrow t$) is shown in Fig. 2. The conversion algorithm slides along the input and output data streams, forward in time. Data is processed in overlapping chunks. In other words, after a block of processing, the sliding part of Fig. 2 shifts slightly to the right. In proportion to the amount of shift, new input stream is exposed and new output stream is completed. The I/O streams are low-bandwidth compared to the compute-intensive processing block.

There are two use cases: demodulation and modulation. For demodulation ($\tau \rightarrow t$), the input stream is in the quantum time domain and the output stream is in the relative time domain. The downsampler decimates the input by 1:m, where decimation factor m is exponentially swept upward from or downward to 1.0. The "warp factor" is the growth rate in m. The input stream consists of real numbers. The FFT performs a real-to-complex FFT to produce a warped spectrum which is treated as a time-domain envelope of magnitude and phase information. To un-warp the spectrum, the upsampler interpolates it by 1:m where

Fig. 3. Demodulation data flow

TABLE 1
Memory regions X, Y, U, and V in Fig. 3 are working buffers. For a 1k
RFFT computed in place, the total is 11kB:

Buffer	Size	Bytes	Usage
X	2048 x 16	4k	Input buffer
Y/U	1024 x 24	3k	FFT working buffer
V	512 x 64	4k	Output buffer

decimation factor m is exponentially swept upward to or downward from 1.0. The output stream consists of vectors that are many accumulations of overlapped upsampler results.

For modulation $(t \to \tau)$, the input stream is in the relative time domain and the output stream is in the quantum time domain. The downsampler decimates the input by 1:m, where decimation factor m is exponentially swept upward from or downward to 1.0 and the resulting spectrum ranges from about N/5 to N/2. The "warp factor" is the growth rate in m. The input stream consists of complex numbers. The IFFT performs a complex-to-real IFFT to produce a time domain envelope. To warp the it, the upsampler interpolates it by 1:m where decimation factor m is exponentially swept upward to or downward from 1.0. The output stream consists of many accumulations of overlapped upsampler results.

The usual use case is demodulation. Modulation could be for testing, reconstruction or extrapolation of a signal, or modulation of an energy source for yet unknown applications.

3 QT DEMODULATION

Multiple demodulator instances can be placed in an FPGA or ASIC to demodulate a large number of ω values in parallel. This would be used in spectral analysis, for finding signals; and deep data mining, for analyzing weak signals. Due to the low I/O bandwidth, the algorithm lends itself to parallelism without the complexity of high-speed signaling or memory management. A low-cost ASIC would be feasible for consumer applications.

The mathematics of signal conversion, besides FFT, is College Algebra. The algorithm can be coded by a typical programmer or engineer with some help from the following derivations.

TABLE 2
High values of M/N are undesirable because of excess processing time
and memory usage. The point of diminishing returns for M/N is
between 2 and 4.

M/N	$Max|R|$	$y_{max} : y_{min}$
2	1.256	3.51:1
4	2.337	10.35:1
8	4.229	68.66:1

3.1 Downsampling

The downsampling process of Fig. 3 translates the sample pitch of X to the sample pitch of Y using an exponential sweep. In the industry, this is known as exponential time-warping.

An exponential chirp sweeps from f_0 to f_1 in a time T. M points of X get mapped onto N points of Y, where $M > N$. Let R be a scaled version of ω for use in the exponential warp and α the X input sample rate in samples per second. Given a particular R and N, M and ω may be calculated. Let $\epsilon = (f_1/f_0)^{1/T}$. The frequency with respect to time is:

$$f = f_0 \cdot e^{\epsilon t} \tag{6}$$

3.1.1 Math

The period of the incoming chirp changes exponentially with index n of $X[n]$. Let $y = e^{|R|/N}$ be the pitch that accumulates along X. It has units of "e's per sample". As a scale factor, let $\omega = \frac{\alpha R}{N}$, in units of "e's per second" e/s. M is the number of input samples warping onto N points. To time-warp the input, let N be a sum of M segments whose size starts at 1 and get compressed exponentially. The calculation of M starts with a geometric progression in Eq. 7.

$$N = \sum_{k=1}^{M} e^{-|R| \cdot (k-1)/N} = \frac{1 - e^{-|R| \cdot M/N}}{1 - e^{-|R|/N}} \tag{7}$$

$$M = \frac{-N}{|R|} \cdot ln\left(1 - N(1 - e^{-|R|/N})\right) \tag{8}$$

An upper limit of 2 for M/N is reasonable from both a mathematical and hardware standpoint. For example, if M is constrained to 2N, N=1024, and α = 10000 samples/second, then $|\omega|$ ranges between 0 and 12.26 e/s. When fixed-sized memories are used, smaller N allows for larger M/N, larger R, and higher ω per input sample rate.

Re-sampling is done on N points (of Y) at a time where the respective indices of X and Y are δ and i. The time span is from 0 to i/N where i sweeps from 0 to N-1 and N is the number of samples. Let λ be the sample pitch of X. It will increase or decrease exponentially and should have a minimum value of 1.0, but allowed a minimum value of less than one to allow for rounding error.

This causes a chirp of matching R to be re-sampled to the upper frequency (either f_0 or f_1 depending on the sign of R). Given output index i, input sample index $\delta(i)$ is the accumulated sum of $\lambda(i)$ when λ starts at 1.0 and increases exponentially or starts at e^{-R} and decreases exponentially. The exponential sweep can be implemented with a multiplier. For each step:
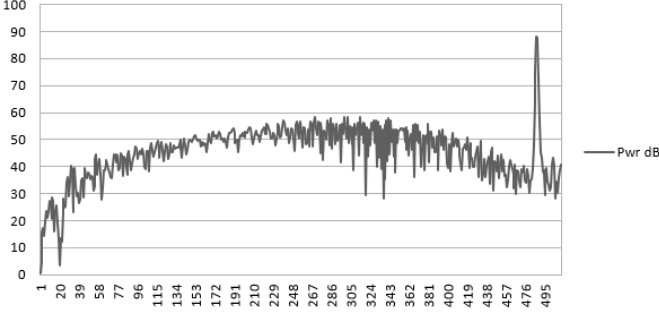
$$\lambda = \lambda + (\lambda \cdot \Lambda) \tag{9}$$

Fig. 4. Power spectrum of U, time-warped test chirp

Fig. 5. Sum of X_δ for downsampling

Fig. 6. X buffer usage

The initial value of λ is e^{-R} when $R < 0$; otherwise, it's 1. The "repeated multiply" approach to exponential sweep is nearly base e, but it needs a small correction factor to hit e. Setting $e^R = (1 + \Lambda)^N$,

$$\Lambda = e^{R/N} - 1 \tag{10}$$

As a sanity check, a downward-chirping sine wave was generated using a phase angle proportional to $e^{n \cdot R/N} - 1$ with index n starting from 0. Λ was set to $e^{R/N} - 1$, where $R = -0.5$ and $N = 1024$. An FFT (with Hann window) was performed on the de-chirped wave to produce the expected narrow peak. The warping process also generates a noise floor about 30 dBm below the peak as seen in Fig. 4. Lower N generates more noise.

3.1.2 Interpolation

The i index is stepped from 0 to N-1, where N is a power of 2 (although it doesn't have to be) for the convenience of the FFT. $\delta(i)$ sweeps non-linearly from 0 to M. For each X, its index δ is the running sum of λ. For each Y point, the downsampler averages one or more X points.

There are two ways to do handle downsampling: Linear interpolation of the output of a variable frequency low pass filter, and summation of λ input samples.

The most common downsampling method is the low pass filter whose output is sampled less often than its input rate. This method attenuates alias frequencies before they make it to the output. Anti-aliasing is good to have, but not essential in this case. Since the alias of an exponential chirp is no longer a pure exponential chirp (it's a linear combination of factors), it will show up in the data stream as wideband noise rather than narrowband interference. A low pass filter might not be needed. The computing resources for the filter aren't cheap. However, a filter would improve SNR. Such a filter must have a linear phase response. A neat trick to use with IIR filters is forward-backward filtering, which zeros the phase shift. The endpoints of the filtered X are allowed some slop, as the Hann window will lop them off anyway.

The non-filter approach is to simply sum λ input samples of X. Some fractional arithmetic is required to handle partial contributions. Fig. 5 illustrates a simple interpolation that adds two fractional endpoints to 0 or more midpoints for downsampling. k is the integer part of δ.

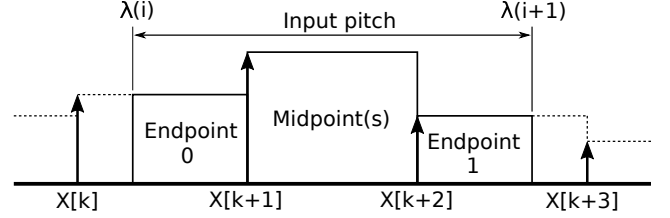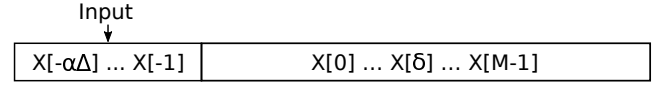In either case, the output of the downsampler could be scaled by $s = \sqrt{1/\lambda}$ to flatten the noise floor. The Central Limit Theorem reduces noise by the square root of the number of samples in a sum. On the other hand, one might expect energy conservation to cause the amplitude of the incoming signal to fall off with time spreading. So, the scaling should be optional. Another instance of exponential sweep, with $\Lambda_s = -\Lambda/2$ and $s_0 = e^{R/2N}$, can produce this scale factor rather easily.

Oversampling would normally use a sliding window on a circular buffer sized as a power of two to allow pointer wrapping by bitwise-and. Fig. 6 shows the memory layout of X. After a block of processing, $\alpha\Delta$ input samples are concatenated to X and the index of X_0 is offset by $\alpha\Delta$, where Δ is the time interval of the blocks.

3.1.3 Testing

The downsampling process is tested and/or calibrated with the aid of the FFT. X memory is initialized with an exponential chirp of rate R where the frequency sweeps from f_0 to Let x be amount of time elapsed. For example, 10.5 represents 10.5 samples.

$$f_1/f_0 = e^{x \cdot R/N} \tag{11}$$

A convenient test is a 2:1 sweep so, for example, you could look for the FFT result's peak to shift in index from 100 to 200 when x is changed from 0 to $ln(2) \cdot N/R$.

Choose f_0 such that the resulting peak lands on an exact integer index. If f_1 is a little off due to implementation details, tweak the initial pitch to center f_1 on the desired FFT result index.

3.2 FFT

After X is time warped into Y, Y is processed by a Fast Fourier Transform and converted to data set U containing N/2 frequency bins. Y and U may share the same physical memory if the FFT is performed in place.

Polar format is preferred for the output of the FFT, for the benefit of the upsampler. A Hann window $w(n)$ is applied to Y before performing the FFT.

$$w(n) = \frac{1}{2}\left(1 - cos\left(\frac{2\pi n}{N - 1}\right)\right) \tag{12}$$

The reference VHDL implementation uses a pipelined CORDIC to perform the FFT. It also applies a Hann window

to Y, converts to polar output, and is shared with the correlator to perform polar to rectangular conversions.

A DIT FFT is the usual choice for RFFT since bit reversal is easier at the input. With an RFFT, you get twice the outputs given real-only input. Adjacent input samples are grouped as pairs, with even samples as real and odd samples as imaginary components of the complex input points. After a CFFT is performed, a separation step doubles the output size. Our experience is that the precision of the separation step degrades with small N (maybe we did it wrong), so a simple CFFT (with zeroed imaginary part) may be preferable in cases of small N.

An FFT can be converted to IFFT somewhat trivially, so the same hardware can support either modulation or demodulation.

3.3 Upsampling

U is upsampled to form time-domain signal V. Let ϵ and j be the respective indices of U and V. For every index ϵ of U, the corresponding frequency can be normalized to Fs/2.

It's much easier to work in terms of exponents than logs, so the preferred re-mapping (another exponential time-warping operation) extracts $U[\epsilon]$ from a linear progression of $V[j]$. Warp indexing uses the relation:

$$\epsilon = \left(\frac{N}{2} - 1\right) e^{\omega(t-\tau)} \tag{13}$$

Time t (scaled to match the output stream's sample rate) sweeps from τ in the opposite direction of R's sign, causing the exponent to start at 1 and decay downward.

Up-sampling $U[\epsilon]$ to $V[j]$ can't use the popular interpolation scheme (zero stuffing) because the interpolation factor must be irrational. Instead, partial contributions to $V[j]$ are extracted from one or two U points by interpolation.

j sweeps downward from $N/2 - 1$. Index $\epsilon(j)$ is independent of R.

$$\epsilon(j) = \left(\frac{N}{2} - 1\right) e^{-kj/N} \tag{14}$$

The desired difference between $\epsilon(0)$ and $\epsilon(1)$ in Eq. 14 is 1. $\epsilon(0) = N/2 - 1$.

$$\epsilon(1) = \frac{N}{2} - 2 = \left(\frac{N}{2} - 1\right) e^{-k/N} \tag{15}$$

This gives a k of approximately 2. The exact value is:

$$k = N \cdot ln\left(\frac{N-2}{N-4}\right) \tag{16}$$

As a sanity check of Eq. 14, $\epsilon(j)$ starts at (N/2-1) which points to the highest frequency element of the FFT result. It decays toward 0 but will never get there. The number of elements in W memory is slightly less than N/2 to allow some I/O headroom. Due to the limited size of W memory, the lowest frequency is about $(1/e)$ of the highest frequency, leaving the lower $\approx 37\%$ of the spectrum unused.

The exponential decay of ϵ can be handled by repeated multiplication, one per $U[\epsilon]$ fetch. The exponential sweep needs a small correction factor to have a base of exactly e. Setting $e^{-k} = (1 + \zeta)^N$,
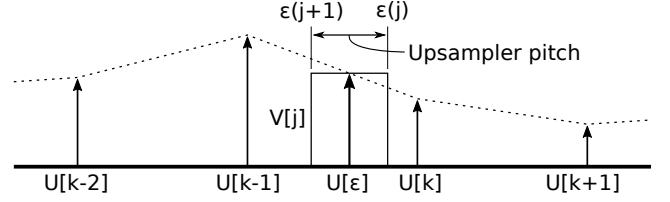
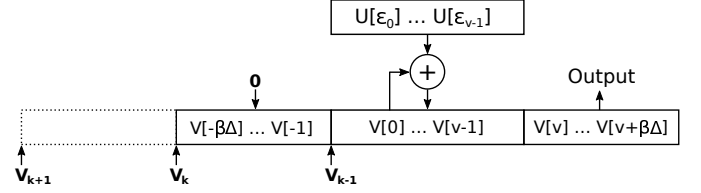$$\zeta = e^{k/N} - 1 \tag{17}$$

Fig. 7. Extraction of U_ϵ

Fig. 8. Correlation of V

Let H_X be the integer number of new X samples (γ) per conversion.

Let H_V be the integer number of output samples per conversion.

$$\gamma = H_V \cdot \frac{k}{|R|} \tag{18}$$

$$H_X = round(\gamma) \tag{19}$$

k is tweaked to allow an integer value for H_X. For a desired $|R|$, pick an integer value for H_V and calculate the closest integer H_X. Adjust k to compensate for the difference between H_X and γ.

Fig. 7 shows upsampling of U to V. It uses linear interpolation to construct a curve to extract from. In this case, the upsampler input pitch is less than 1.0 samples. The height of U_ϵ is interpolated and multiplied by the pitch to get the area under the curve, to be added to V[j]. The operation is similar to the "$\lambda < 1$" case of downsampling, so the same hardware can support downsampling and upsampling.

Since ϵ is always positive, the upchirp case of $R > 0$ needs to have its j index mirrored by using V[v-j], where v is the maximum j such as (15/32)N. The upsampler output is added to V memory as described below, indexed from the top or bottom of the active region of V.

3.4 Correlation

Warped U is added to output buffer V by RMS summation, staggered in time (by H_V samples) for each processing block. When the downsampler's R value matches the chirp rate of an incoming chirp, multiple peaks in the warped FFT output correlate in the output stream to produce a corresponding output pulse in the V stream. A more complex signal such as overlapping and/or modulated chirps will produce pulse trains and/or modulation envelopes in the V stream.

Fig. 8 shows the output correlator, another view of buffer V. The output stream flows from left to right, being initialized to 0 outside the accumulation region. After U_ϵ is added to V, the V_0 index moves H_V points to the left, leaving H_V newly minted output points.

Fig. 9. Modulation data flow

Fig. 10. Interpolation of Y for upsampling
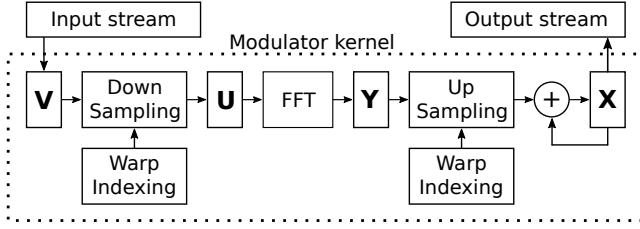
Elements of V are accumulated squares of magnitudes. An attempt was made to accumulate vectors, with the idea that the phase rotations might sync up, but it didn't work in simulation. So, angle data from the FFT is discarded.

4 QT MODULATION

Modulation is the reverse of demodulation. It inputs a stream of (magnitude, angle) vectors and outputs a stream of real samples. The downsample and upsample processes of modulation are the reverse of demodulaton's upsample and downsample processes respectively.

4.1 Downsampling

V is downsampled to form frequency-domain signal U. Eq. 14 relates integer index j to fractional index $\epsilon(j)$. Each point of V can be interpolated into a variable number of U points in a way that accumulates V points and spits out U points as needed.

Another view is easier to describe mathematically, but needs a logarithm. Let ϵ and j be the respective indices of U and V where $\epsilon/j < 1$. ϵ is an integer that steps downward from ϵ_0.

$$\epsilon_0 = \frac{N}{2} - 1 \tag{20}$$

Rewriting equation 14 for $j(\epsilon)$,

$$j(\epsilon) = \left(\frac{N}{2} - 1\right) ln\left(\frac{\epsilon_0}{\epsilon}\right) \tag{21}$$

The minimum ϵ is determined by the span of j. Let j range from 0 to $v - 1$ and $v = 0.469N$.

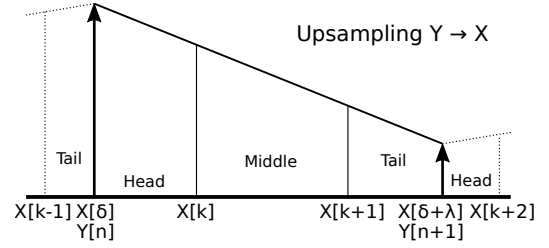$$\epsilon(v - 1) = \epsilon_0 e^{\frac{-(v-1)}{0.5N-1}} \tag{22}$$

$$\epsilon(0.469N) = \epsilon_0 e^{\frac{-(0.469N-1)}{0.5N-1}} \approx 0.391\epsilon_0 \tag{23}$$

Since ϵ is always positive, the upchirp case of $R > 0$ needs to have its j index mirrored by using V[v-j], where v is the maximum j such as 0.469N.

4.2 IFFT

The IFFT ($U \rightarrow Y$) is an Inverse Fast Fourier Transform that translates N/2 complex frequency values to N/2 complex points in the relative time domain. These may be assumed to have Hermitian symmetry, so the imaginary part of Y can be ignored. It's also possible to realize Y as N real points.

A Hann window is applied to Y after the FFT. Y is then warped and accumulated in X in a manner similar to the demodulator's correlation function.

4.3 Upsampling

The upsampling process of Fig. 9 translates the sample pitch of Y to the sample pitch of X using the reverse of the downsampling process.

Fig. 10 illustrates an interpolation scheme for recreating X from Y. The slope calculation requires a $1/\lambda$ scale factor. The expense of division can be avoided by using another instance of exponential sweep such as that described by Eq. 10.

The X points are the trapezoidal area under the curve in Fig. 10. The *Head* and *Middle* regions produce output points. The *Tail* result is carried into the next *Head*.

Summation in X is similar to the data flow of Fig. 8, but a little easier since X and Y are real (rather than complex) numbers. X memory is wider than with demodulation to handle accumulation in memory.

5 TESTING

The demodulation algorithm was tested by coding the algorithm in C (as a console application) and instrumenting it to display variables, save arrays to files, and benchmark the various stages. KissFFT is used as the 1K complex FFT. On a fast Core-i7 PC, the algorithm correlates a frame in about 100 usec. Allowing 100 usec per 32 points amounts to 320K SPS of input which, when $R = -0.5$, is 80K SPS of output.

5.1 EEG data

An ideal test for the algorithm is EEG data taken from public data sets. The DREAMS Sleep Spindles Database at Faculté Polytechnique de Mons (Belgium) TCTS Lab [18] provides EEG data in text format. The "excerpt2" data set consists of 30 minutes of 200 SPS data as well as the stage of sleep for each 5-second interval. Sleep is useful to look at due to the presence of alpha, delta and theta waves. The session has all stages of sleep from awake to REM to stage 4. If exponential chirp spectra are present and forming informational pulse trains, that's an indication that the brain is a receiver where consciousness is experienced. The origin of consciousness is in a timeless, eternal realm.

The demodulation algorithm looks at the signal bandwidth between about $F_S/5$ and $F_S/2$. Many data sets have a region of interest far below the sample rate. Decimation is typically used to lower the sample rate to bring it to the desired region of interest. Decimation by a factor of M usually involves low-pass filtering the signal and taking every Mth data point as output. A more sloppy method is to simply sum each set of M input points and ignore the

aliasing effects since those will be smeared across the noise floor.

The demodulation app processes up to a minute or so of data starting at a beginning time and saves it as a BMP (using colored amplitude) with time on the horizontal axis and R on the vertical. It's feasible to implement just a console application, avoiding GUI work altogether. The BMP is the scientific output, viewable in many media as well as on the web. For an R range of 0.25 to 0.75, there are between 3 and 8 input points per output point. One minute of 200 Hz data produces a BMP that's 4500 pixels wide. A desktop PC has built-in tools for viewing gigapixel images, so size is mostly limited by your patience (time). A 16384 x 2048 image requires 100MB of RAM. Not much to ask of a modern PC.

REFERENCES

[1] E. F. Kelly, *Irreducible Mind: Toward a Psychology for the 21st Century*. Rowman and Littlefield, 2009.

[2] B. S. Dewitt, "Quantum theory of gravity. i. the canonical theory," *Physical Review*, vol. 160, pp. 1113–1148, 1967, doi:10.1103/PhysRev.160.1113.

[3] D. N. Page and W. K. Wootters, "Evolution without evolution: Dynamics described by stationary observables," *Physical Review D*, vol. 27, no. 12, pp. 2885–2892, 1983.

[4] E. M. et al., "Time from quantum entanglement: an experimental illustration," *Physical Review A*, vol. 89, 2014, 052122.

[5] A. C. Lobo, "Time and consciousness in a quantum world," 2017.

[6] J. Li, "A timeless and spaceless quantum theory of consciousness," *NeuroQuantology*, vol. 11, pp. 431–442, 2013.

[7] O. Brunet, "Geometric time and causal time in relativistic lagrangian mechanics," 2016.

[8] D. J. Chalmers, "Facing up to the problem of consciousness," *Journal of Consciousness Studies*, vol. 2, pp. 200–219, 1995.

[9] e. a. Jeanne Achterberg, "Evidence for correlations between distant intentionality and brain function in recipients: A functional magnetic resonance imaging analysis," *Journal of Complementary and Alternative Medicine*, vol. 11, no. 6, pp. 965–971, 2005.

[10] B. Mandelbrot, *The Fractal Geometry of Nature*. W. H. Freeman and Company, 1982.

[11] G. W. Leibniz, *Discourse on Metaphysics*. Open Court Classics, 1686.

[12] E. Milotti, "1/f noise: a pedagogical review," 2002.

[13] A. N. et al, "Nonlinear system identification using exponential swept-sine signal," *IEEE Transactions on Instrumentation and Measurement*, vol. 59, no. 8, pp. 2220–2229, 2010, doi:10.1109/tim.2009.2031836.

[14] T. J. A. Craddock, "Anesthetic alterations of collective terahertz oscillations in tubulin correlate with clinical potency: Implications for anesthetic action and post-operative cognitive dysfunction," *Scientific Reports*, vol. 7, no. 1, p. 9877, 2017. [Online]. Available: https://doi.org/10.1038/s41598-017-09992-7

[15] S. Hameroff, "Consciousness in the universe: a review of the 'orch or' theory," *Physics of Life Reviews*, vol. 11, 2013.

[16] G. Bonmassar and E. L. Schwartz, "Space-variant fourier analysis: the exponential chirp transform," *IEEE Transactions on Pattern Analysis and Machine Intelligence*, vol. 19, pp. 1080–1089, 1997, DOI:10.1109/34.625108.

[17] E. L. Schwartz, "Cortical anatomy, size invariance, and spatial frequency analysis," *Perception*, vol. 10, pp. 455–469, 1981.

[18] S. Devuyst, *The DREAMS Sleep Spindles Database*, 2011 (accessed January 11, 2019). [Online]. Available: http://www.tcts.fpms.ac.be/ devuyst/Databases/DatabaseSpindles/